Automatic detection of avalanches in high-resolution optical satellite data

Results from the ESA avalRS project's feasibility study on automated avalanche detection
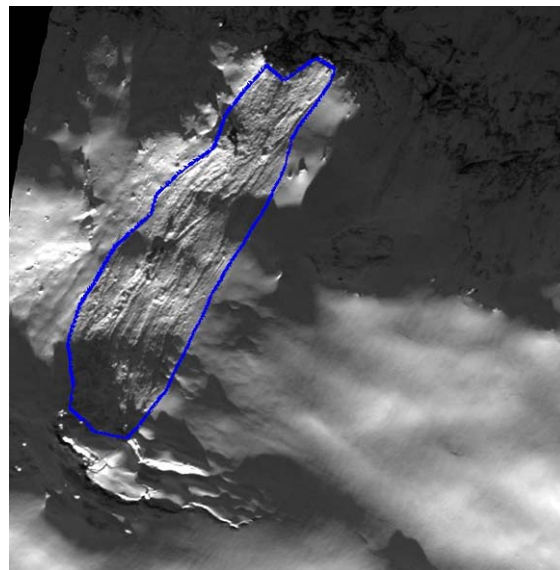
Note no	**SAMBA/04/10**
Authors	**Siri Øyen Larsen, Arnt-Børre Salberg and Rune Solberg**
Date	**21 May 2010**
Contract	**ESRIN/Contract No. 22139/08/I-EC**

Note

Norsk Regnesentral
NORWEGIAN COMPUTING CENTER

Statens vegvesen NGI

Norsk Regnesentral

Norsk Regnesentral (Norwegian Computing Center, NR) is a private, independent, non-profit foundation established in 1952. NR carries out contract research and development projects in the areas of information and communication technology and applied statistical modelling. The clients are a broad range of industrial, commercial and public service organizations in the national as well as the international market. Our scientific and technical capabilities are further developed in co-operation with The Research Council of Norway and key customers. The results of our projects may take the form of reports, software, prototypes, and short courses. A proof of the confidence and appreciation our clients have for us is given by the fact that most of our new contracts are signed with previous customers.

Norges Geotekniske Institutt

NGI (Norwegian Geotechnical Institute) is a leading international centre for research and consulting in the geosciences. NGI develops optimum solutions for society, and offers expertise on the behaviour of soil, rock and snow and their interaction with the natural and built environment. NGI works within the oil, gas and energy, building and construction, transportation, natural hazards and environment sectors. NGI is a private foundation with office and laboratory in Oslo, branch office in Trondheim and daughter company in Houston, Texas, USA. NGI was awarded Centre of Excellence status in 2002 and leads the International Centre for Geohazards (ICG).

NGI is the prime contractor of the project behind the work presented in this report.
Address: Norwegian Geotechnical Institute (NGI), P.O. Box 3930 Ullevaal Stadion, NO-0806 Oslo, Norway
Contact persons: Regula Frauenfelder (regula.frauenfelder@ngi.no) and Kalle Kronholm (kalle.kronholm@ngi.no)

Norwegian Public Road Administration

The Norwegian Public Roads Administration (NPRA) is responsible for the planning, construction and operation of the national and county road networks, vehicle inspection and requirements, driver training and licensing. It is also authorized to grant subsidies for ferry operations. The Public Roads Administration is under the leadership of the Directorate of Public Roads, which is an autonomous agency subordinated the Ministry of Transport and Communication. The Public Roads Administration encompasses five regional offices.

Address: Norwegian Public Road Administration. P.O. Box 8142 Dep. NO-0033 Oslo, Norway
Contact person: Jan-Otto Larsen (jan-otto.larsen@vegvesen.no)

Title	**Automatic detection of avalanches in high-resolution optical satellite data**
Authors	**Siri Øyen Larsen, Arnt-Børre Salberg and Rune Solberg**
Quality assurance	Rune Solberg
Date	21 May 2010
Year	2010
Publication number	SAMBA/04/10

Abstract

We demonstrate that avalanches could be successfully detected and mapped from high resolution optical satellite imagery. The key part of the detection algorithm is a texture segmentation step, which distinguishes the avalanches from other objects such as smooth and rugged snow, trees and rock. Two different approaches are investigated: a method based on gray-level co-occurrence matrices (GLCM), and a method based on directional filters. To further enhance the performance we propose to process the mapped avalanche objects in feature extraction and classification stages.

The algorithms are developed and trained on a Quickbird image of a Norwegian mountain area which contains several avalanches. The segmentation algorithms detect parts of all avalanches. The directional filter method was also tested and validated on another Quickbird image, covering a different scene in Norway. The GLCM approach has a higher rate of false detections than the directional filters approach, but maps the outline of the avalanches better. A brief demonstration of feature extraction shows that context and shape of detection objects may provide important information to further enhance the performance by reducing the number of false detections and refining the outline. From this case study, we believe that avalanche mapping in high resolution optical images is possible.

Keywords	Avalanche mapping, texture, Quickbird
Target group	Remote sensing researcher, avalanche researchers, road authorities
Availability	Open
Project number	220 438
Research field	Earth observation
Number of pages	38
© Copyright	Norsk Regnesentral

Contents

1 Introduction

The main objective of the avalRS project is to provide the Norwegian Public Roads Authority with avalanche inventories based on remote sensing data captured briefly after major avalanche events. The service is to be demonstrated in specific service case areas defined on-the-fly (i.e. depending on where major avalanche events will occur during the project phase) within the mountains of South-, West- and Central Norway.

AvalRS aims at demonstrating that such a service is possible and that it will provide decision support during avalanche-imposed road closures, and to help validate the issued avalanche forecasts. Overview over the affected problem area, specifically the length of the avalanche-affected road section and the volume of snow on the road, are essential for the authorities during road closures.

The avalRS project is a joint project between the Norwegian Geotechnical Institute (prime contractor), the Norwegian Computing Center (sub-contractor) and the Norwegian Public Roads Authority (end-user). The project is funded by the ESA DUE (Data User Element) Innovator II programme (Contract No. 22139/08/I-EC).

Each year, dry and wet snow avalanches hit populated areas and parts of the Norwegian transport network in the mountain regions of Norway, leading to the loss of lives and the damaging of buildings and infrastructure. When avalanches hit a road the goal of the authorities is to reopen the road as fast as possible. To do this they must first obtain an overview of the problem, specifically the length of the avalanche-affected road section and the volume of snow on the road. Traditionally, this has been done by flying over the assumed affected stretch of road with a helicopter. This method has the following two major drawbacks: 1) flight reconnaissance must be possible, i.e. the weather must permit good visibility and relatively low wind speeds. After a snow storm it may typically take some time, often several days, before such conditions are fulfilled, 2) a helicopter flight may give good information along the (linear) flight path but does not give a good spatial cover age of an area.

Satellite based remote sensing may remedy these drawbacks and act as an additional source of information for the road administration (NPRA) immediately after road closures.

In the literature, only the work by Bühler et al. (2009), has considered automatic detection of avalanches using remote sensing data. Bühler et al. (2009) proposed a methodology for automated detection and mapping of avalanche deposits in the Swiss Alps using optical aerial imagery. A processing chain integrating directional, textural and spectral information was proposed, and though certain limitations exist, encouraging detection and mapping accuracies was reported.

We will also, as Bühler et al. (2009), apply texture as a feature for detection and mapping avalanches, but our approach will be designed for high resolution satellite based imagery. Texture has often been utilized to segment and classify objects in images (Fogel and Sagi, 1989; Jain et al., 1997; Haralick et al., 1973; Varma and Zisserman, 2004). To detect and map the avalanches, we demonstrate two different texture segmentation methods; one based on gray-level co-occurrence matrices (Haralick et al., 1973) and one based on directional filters (Varma

and Zisserman, 2004). In particular, for directional filters, we will utilize that the avalanche textures are oriented in the same direction as the aspect of the terrain. Even if the texture segmentation is efficient in order to detect potential avalanche segments, further processing is necessary in order to reduce the number of false detections and to refine the avalanche mappings. We therefore propose to extract shape and context features from the detected objects, in addition to texture features, and perform an object based classification of the detected objects. Such approach has been applied successfully in other projects NR has carried out on pattern recognition in satellite data, including oil spill detection in radar images (Solberg et al., 2007) detection of remains of cultural heritage in optical imagery (Trier et al., 2009) and detection of vehicles in optical imagery (Larsen et al., 2009).

NR🌐 **Automatic detection of avalanches in high resolution satellite data**

2 The general approach

In other projects with similar type of challenges, i.e., automated object detection from satellite images, we have obtained good results using an approach consisting of image segmentation into objects, followed by feature extraction and classification (Figure 2-1). Examples include oil spill detection in SAR images (Solberg et al., 2007), and detection of cultural heritage sites (Trier et al., 2009) or vehicles (Larsen et al., 2009) in high-resolution optical images. We propose using a similar approach for automated avalanche detection and mapping. Each processing step must of course be adjusted to meet the requirements for object recognition of the specific type, here the objects are avalanches.
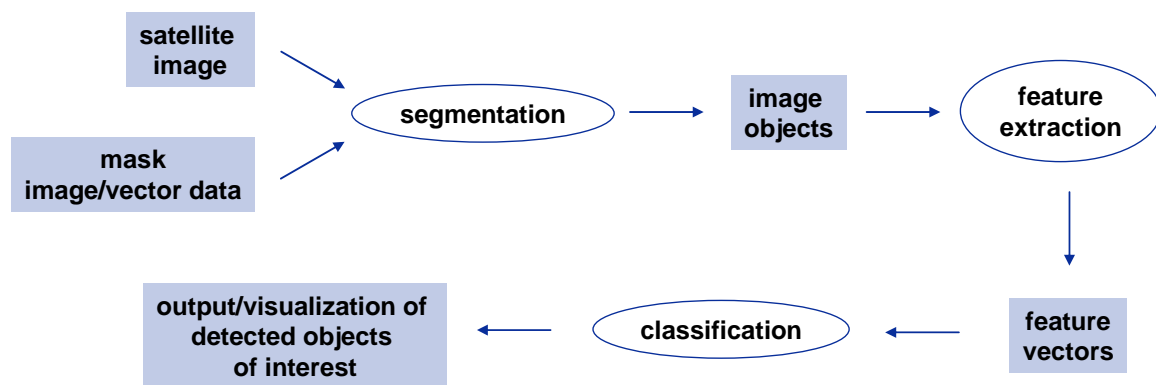
Figure 2-1. Processing flow of the general approach.

3 Experimental data set

Initially, two SPOT images were ordered from the Tyin area in central Norway. The images were acquired February 12 and 15, 2008, about two weeks after several large avalanches were released in the period of January 24-26. The pixel resolution of the images is 20 m. The images were orthorectified using a digital elevation model (DEM) of 25 m resolution together with manually selected ground control points. There are no weather stations on site, but the nearest weather stations showed some snow fall in the first week of February. It was not possible to visually detect the avalanches in the SPOT images, most likely because the resolution is too coarse, although weather conditions between the event and image acquisition also seem to have played a role. Further details on this are reported in the Service Demonstration Document of the project (cf. Frauenfelder et al., 2010).

We have analyzed one QuickBird image from the Hellesylt area, also Central Norway, acquired on April 16, 2005 (Figure 3-1), and one QuickBird image from the Dalsfjorden area, acquired on April 3, 2005 (Figure 3-2). Several avalanches are visible in the images, which has a resolution of 0.6 m in the panchromatic band and 2.4 m in the multispectral bands (blue, green, red, and near-infrared). The avalanche detection methods are developed on the Hellesylt image, and all training data needed is also extracted from this image. The Dalsfjorden image is used as a validation/demonstration image, in sense that all processing of the Dalsfjorden images is performed using methods and training data extracted from the Hellesylt image.
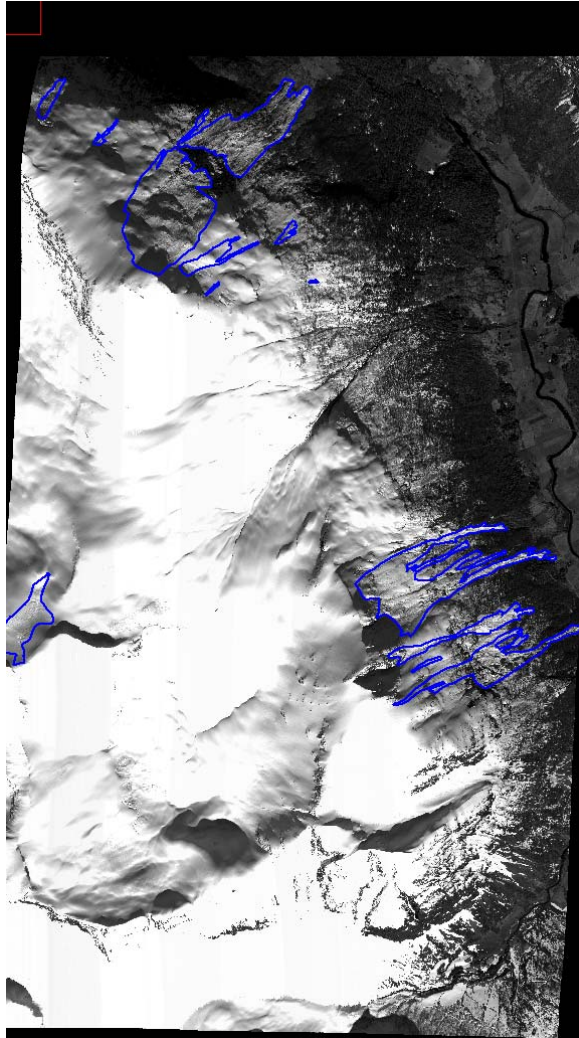
Figure 3-1. Panchromatic QuickBird image over the Hellesylt area. Avalanches are outlined in blue. Source: Norwegian Geotechnical Institute
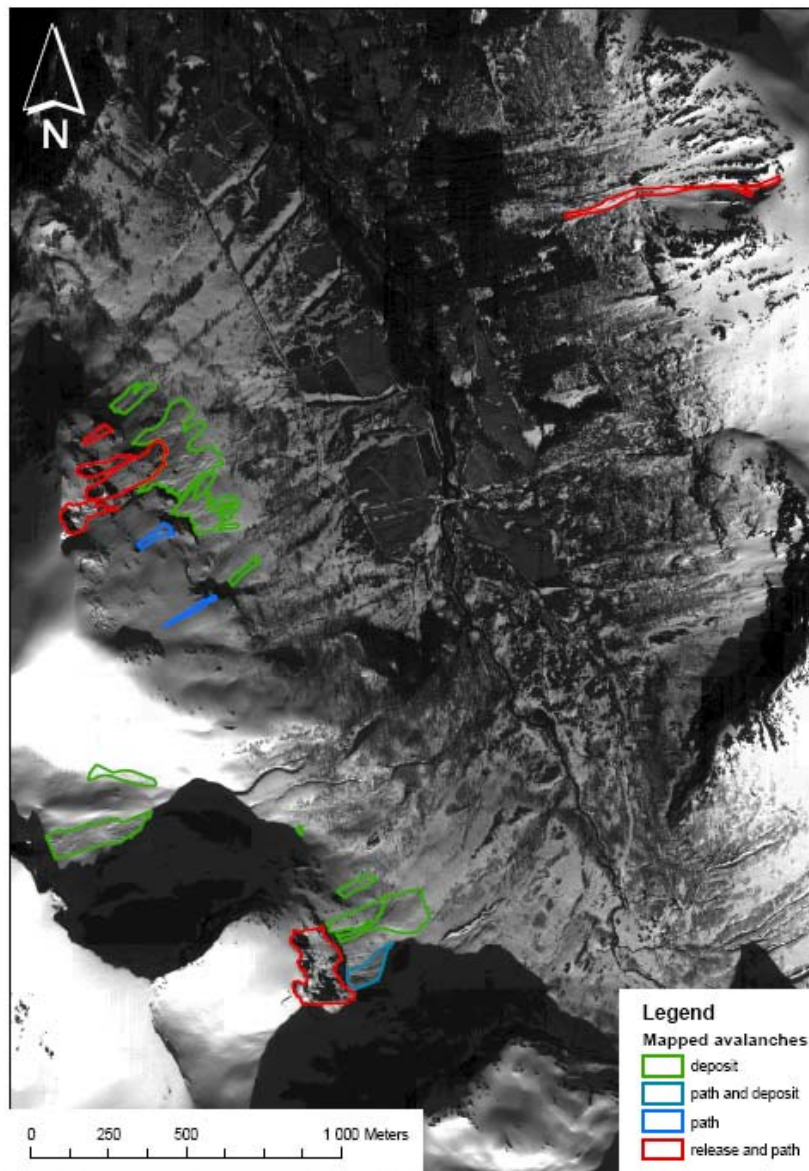
Figure 3-2: Panchromatic QuickBird image over the Dalsfjorden area. Source: Norwegian Geotechnical Institute

For experiments, the Hellesylt image was orthorectified using a 15 m resolution DEM and manually selected ground control points. We used the built-in ENVI function for orthorectification. This tool also takes into account some sensor specific parameters. Slope and aspect images with resolution corresponding to the panchromatic image were also calculated based on the 15 m DEM. Orthorectification using a 25m resolution DEM were also investigated, but the due to the high resolution of the Quickbird images the results were not sufficiently accurate.

Forest and agriculture masks are extracted from a GIS vector layer (1:50'000) describing area resource classes (AR50 data) provided by The Norwegian Forest and Landscape Institute (Norsk institutt for skog og landskap).

4 Segmentation of avalanche structures

Two different segmentation strategies have been tested: texture based segmentation and segmentation based on directional filters. The two strategies will be described in Sections 4.1 and 4.2, respectively.

4.1 Texture based segmentation

Texture is one of the important characteristics that make it possible to visually discriminate avalanche affected areas from non-affected areas in the image. Our first attempt is to use textural measures for segmentation. This approach is inspired by Bühler et al. (2009), who present a methodology for automated detection and mapping of avalanche deposits in the Swiss Alps using optical aerial imagery. We will shortly summarize Bühler's approach, before we describe our work.

Bühler et al. first exclude regions not affect by avalanches based on three different criteria: 1) The numerical simulation tool RAMMS (developed at WSL Institute for Snow and Avalanche Research SLF in Switzerland), which predicts the potential area affected by avalanches, based on automatic derivation of starting zones from digital elevation data. 2) Slopes with an inclination (derived from a digital elevation model) of 35° or more are excluded, since it is unlikely that an avalanche stops its flow within steep slopes, and their method aims to locate avalanche deposits only. 3) Areas not covered by snow are excluded using spectral thresholding. Next, they use the gray level co-occurrence matrix to compute textural measures from the Normalized Difference Angle Index (NDAI), which is computed using multidirectional, near-infrared (NIR) image data, more specifically, using nadir and backward looking NIR bands. The entropy, which is one of the textural measures, is then thresholded to extract rough snow surface areas, and an object-based classification approach is used to separate avalanche deposits from other rough surfaces. The detected avalanches are separated in three classes depending on their dimension.

As we are going to detect all avalanche affected areas, including starting zones, we do not want to exclude steep slope regions. Nor do we exclude snow free areas based on spectral thresholding, mainly because it is difficult to find an appropriate threshold in the Hellesylt image, due to varying illumination conditions, shadows, etc.

We compute various textural features from the panchromatic image based on Haralick's approach (Haralick et al., 1973), using the gray-level co-occurrence matrix (GLCM). This matrix describes the gray-level intensity variation between pixels located with a given direction and distance with respect to each other. The distance and direction can be specified using offsets in the x- and y-directions, i.e., $(\Delta x, \Delta y)$. The gray levels must be quantized to L levels, say $\{1, ..., L\}$. Given an MxN image I, the GLCM can be defined as the LxL-matrix $P_{\Delta x, \Delta y}$ whose (i,j)'th entry is given by

$$P_{\Delta x,\Delta y}\left(i,j\right)=\sum_{p=1}^{M}\sum_{q=1}^{N}\begin{cases}1, & if\ I(p,q)=i\ and\ I(p+\Delta x,q+\Delta y)=j\\0, & otherwise.\end{cases}$$

Equation 4-1. Gray-level co-occurrence matrix.

Haralick et al. suggest a set of 28 textural features which can be extracted from the GLCM, one of which is the entropy, defined as

$$- \sum_{i=1}^{L} \sum_{j=1}^{L} p(i, j) \log p(i, j),$$

Equation 4-2. Entropy.

where p is the normalized version of the GLCM, i.e., $p(i,j) = P(i,j) / (\Sigma_{i,j} P(i,j))$. For many applications, such as ours, it is natural to compute one GLCM for each pixel neighbourhood in the image, since the image consists of many different textures. The textural features can then be defined in each pixel using a GLCM computed in a neighbourhood centered at this pixel.

We compute eight different textural features over the image using the built-in ENVI function for texture based co-occurrence filters, which is consistent with the Haralick-approach. These eight features are: mean, variance, homogeneity, contrast, dissimilarity, entropy, second moment, and correlation (cf. (Haralick et al., 1973) for the specific formulas). We experiment with different values of Δx and Δy and different sizes (M,N) of the neighbourhood image for the GLCM computations, and found that suitable values are $M=N=9$, $\Delta x=1$, and $\Delta y=-1$. For gray level quantization, we apply the default value $L=64$. The small values of Δx and Δy indicate that the texture information is contained in the neighbouring pixels of a given pixel.

For illustration of some of the features, the entropy and homogeneity images are shown in Figure 4-1, and the correlation and variance images are shown in Figure 4-2. Note that the entropy is well suited for extraction of avalanche affected areas (cf. avalanche outlines in Figure 3-1), as these areas have high entropy. Unfortunately, there are other areas with high entropy as well. These areas correspond to sparse forest or areas with large intensity variations due to material changes or shadows; see Figure 4-3 for some examples.

Before thresholding, we apply a forest mask, i.e., we exclude forested regions, as avalanches are not likely to be present in dense forest. The entropy image is thresholded using the threshold

$$t_{high\ entropy} = \mu_{non\text{-}forest} + 1.7 \sigma_{non\text{-}forest},$$

where $\mu_{non\text{-}forest}$ is the mean entropy of the pixels not included in the forest mask, and $\sigma_{non\text{-}forest}$ is the corresponding standard deviation. This threshold was found based on trial and error as a compromise between not including too many non-avalanche pixels while at the same time including as many avalanche pixels as possible. After thresholding (entropy image $> t_{high\ entropy}$) we extract the high entropy segments, i.e., each connected set of foreground pixels. Segments whose area is less than 1000 pixels ($=360\ m^2$) are discarded. However, this threshold was chosen by inspecting a single Quickbird image. If more images are available, the threshold may need to be adjusted.
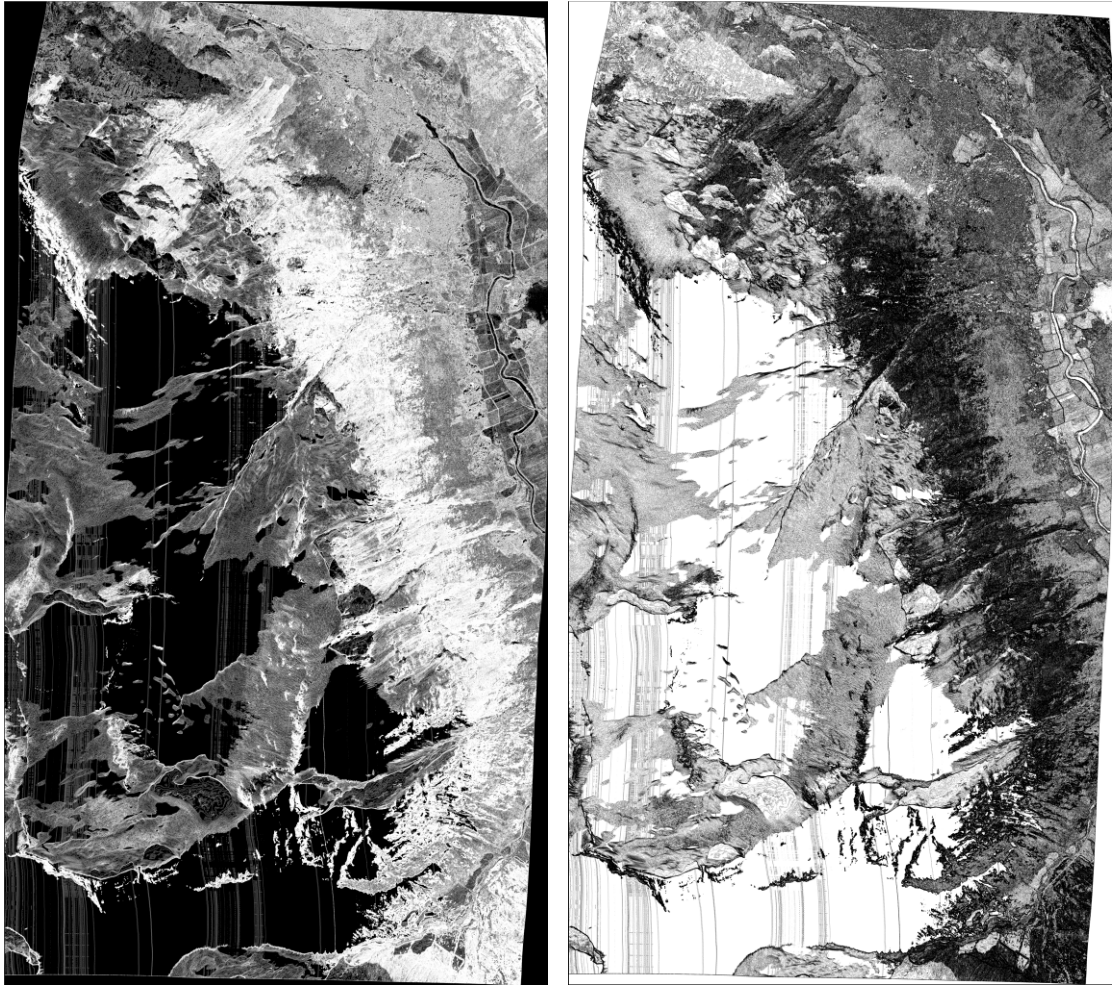
Figure 4-1. Entropy (left) and homogeneity (right). Dark areas correspond to low entropy and low homogeneity, whereas light areas correspond to high entropy and high homogeneity.
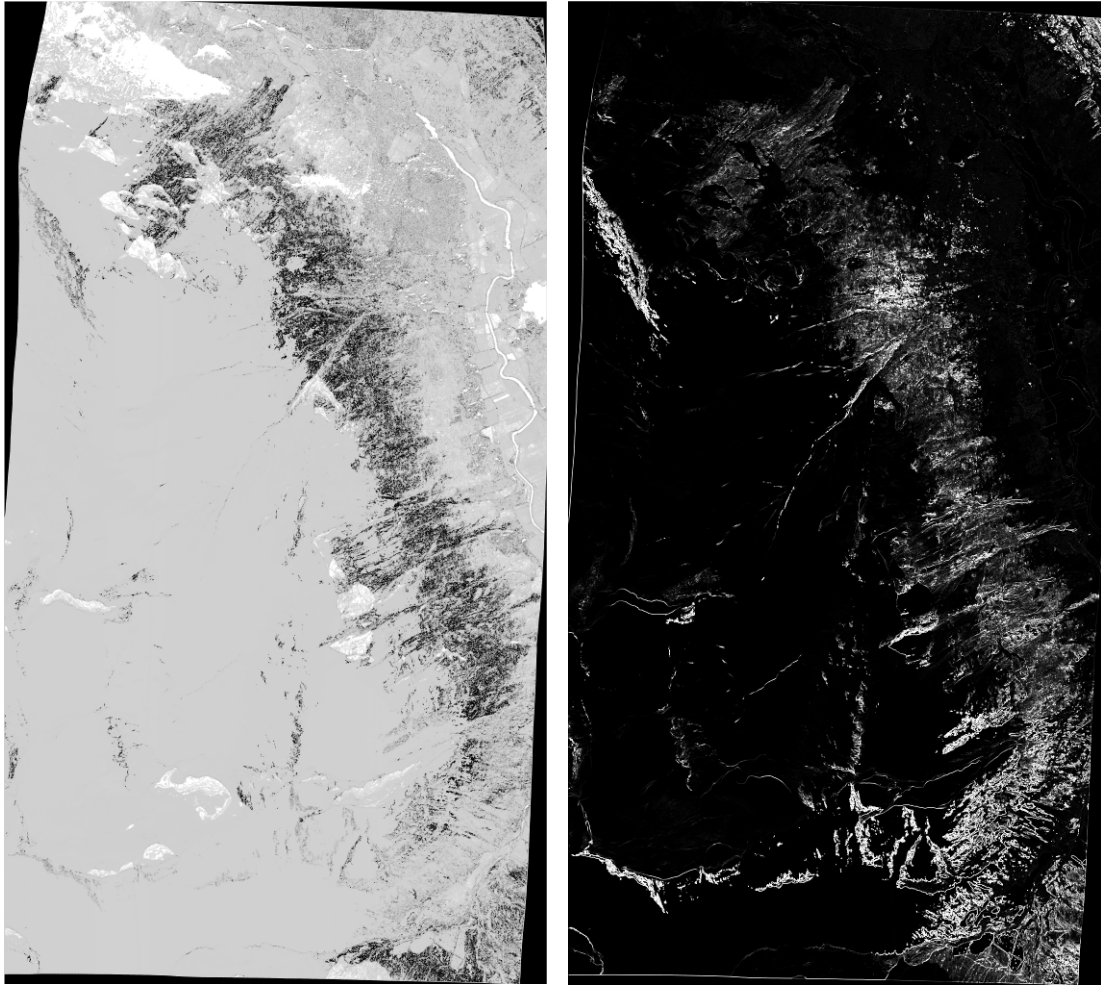
Figure 4-2. Correlation (left) and variance (right). Dark areas correspond to low correlation and low variance, whereas light areas correspond to high correlation and high variance.

NR **Automatic detection of avalanches in high resolution satellite data**
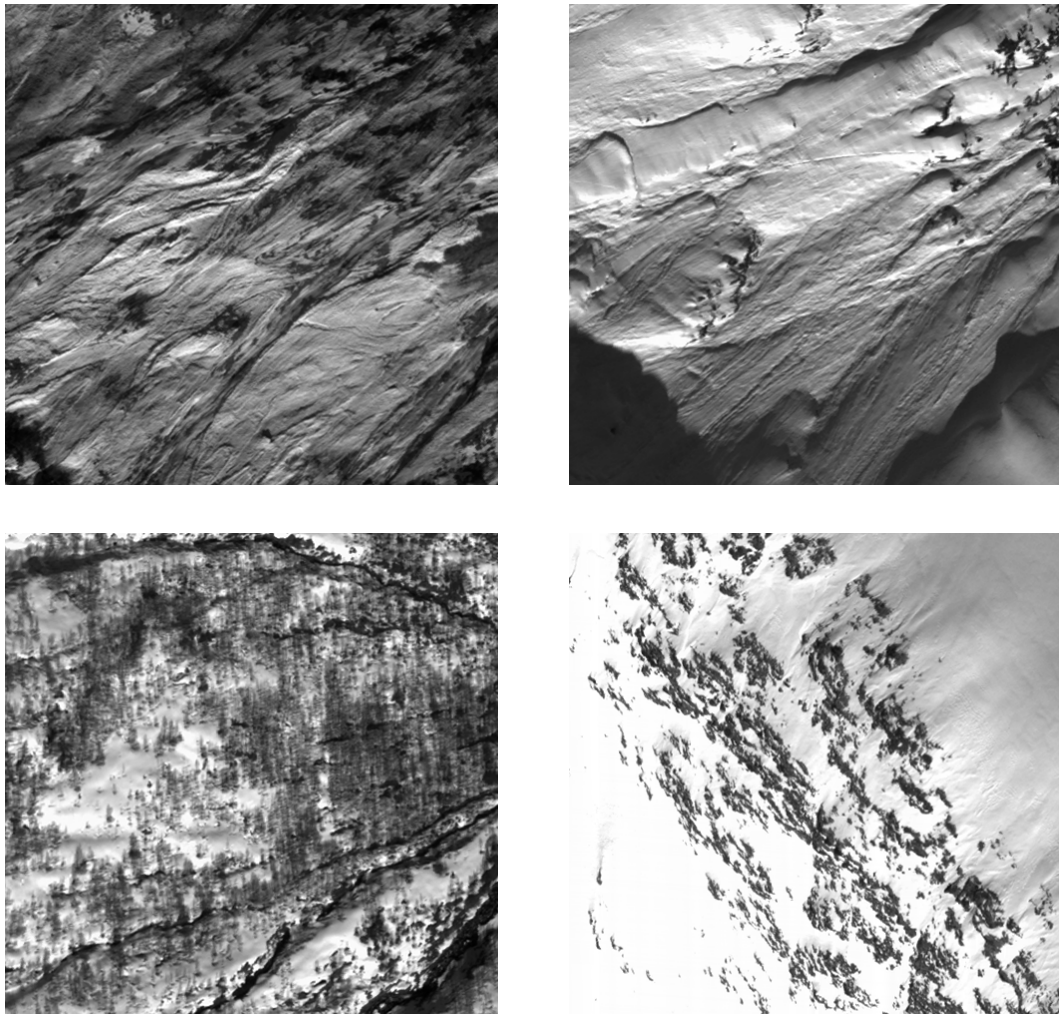
Figure 4-3. Examples of high entropy areas. Both the upper images are extracted from avalanche affected regions. The image below on the left is extracted from a sparse forest area, while the image below on the right is from an area with large intensity variations due to material changes between dark stone and bright snow.

4.2 Avalanche segmentation using directional filters

Extracting textural features by convolving the image with a given filter is often applied in texture segmentation and classification (see e.g., Varma and Zisserman, 2004; Fogel and Sagi, 1989; Bovik et al., 1990; Jain et al., 1997). Typically, a set of convolved images are created by applying a bank of filters, each with given characteristics (e.g., scale, orientation, frequency, etc.). Then each filtered image is combined into a multi-dimensional image, which is further analyzed to stratify the image into segments with similar texture patterns.

The approach we apply is based on the work by Varma and Zisserman (2004). First we select a set of region of interests (ROIs), each corresponding to the following texture types or content classes: *avalanche, smooth snow, rugged snow, sparse trees,* and *rock.* We do not select ROIs corresponding to dense forest and agriculture areas since forest and agriculture masks are available.

In the learning stage, each ROI is convolved with a filter bank to generate filter responses. The filter responses corresponding to the same class are then clustered using a K-means clustering algorithm, and the resulting cluster means are chosen as *textons* (Figure 4-4). For each class, 10 textons are generated, resulting in a dictionary of a total of 50 textons. The corresponding cluster covariances are also estimated, and each pixel in the training ROIs are labelled by classifying each pixel to one of the textons using a maximum likelihood classifier based on a Gaussian distribution. The histogram of texton frequencies is then used to form *models* corresponding to the training ROIs (see Figure 4-5). To perform a segmentation or pixel classification of the image we create a texton map of the whole image by classifying each pixel. Then, for each pixel, we select a local neighbourhood, compute the texton histogram, and then compare with the models learnt during training (Figure 4-6). A nearest neighbour classifier is used and the χ^2 statistic is employed to measure the distances. The histograms are normalized to sum to unity.
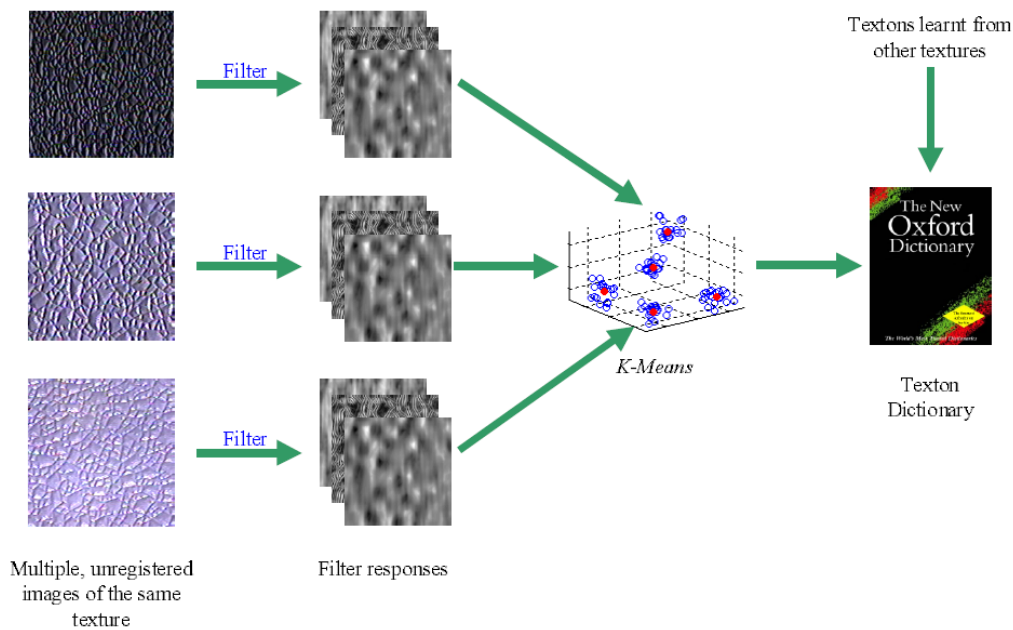
Figure 4-4. Generating the texton dictionary. Figure taken from Varma and Zisserman (2004).
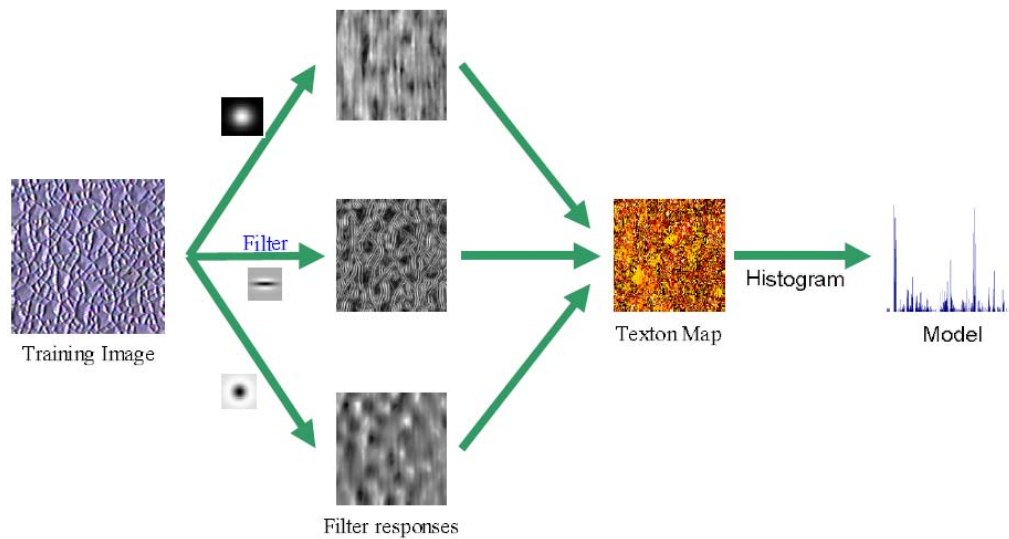
Figure 4-5. Model generation. Figure is taken from Varma and Zisserman (2004).
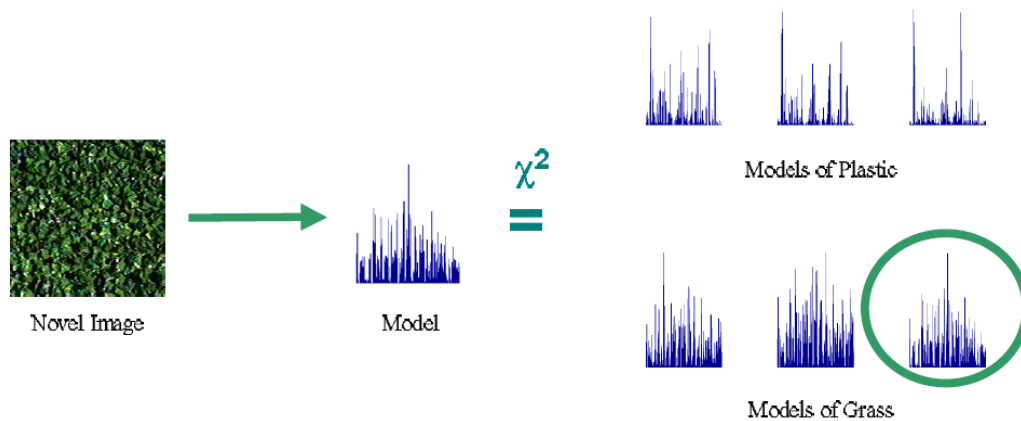
Figure 4-6. Model classification. Figure is taken fra Varma and Zisserman (2004).

The filter bank we apply is based on the so-called MR8 filter bank (Varma and Zisserman, 2004). The MR8 filter bank (Figure 4-7) consists of 38 filters but only 8 filter responses. The shape of the filters is determined by scale parameters, and the filters may be designed to enhance linear structures. The filter bank contains filters at multiple orientations but their outputs are "collapsed" by recording the maximum filter response across all orientations. An avalanche typically results in a texture pattern that has linear structures in the same direction as the aspect of the hill side. We have therefore modified the MR8 filter bank approach by selecting the same orientation of the filters as the aspect of the DEM. Furthermore, since trees and tree shadows are oriented vertically in the image, we extend the MR8 filter bank by including 6 filters with vertical orientation. Hence, our resulting texture segmentation is based on a 14 dimensional image. The scale parameters selected are (1.5, 3.0, 6.0) and (0.5, 1.0, 2.0) for the major and minor axis of the directional filters. The scale parameter for the isotropic filters is 5.0.
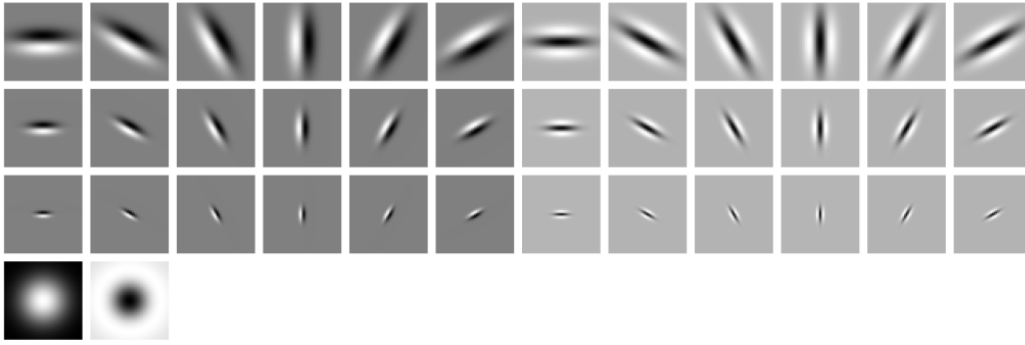
Figure 4-7. The MR8 filter bank. Figure is taken from Varma and Zisserman (2004).

NR🌐 **Automatic detection of avalanches in high resolution satellite data**

5   Feature extraction and classification

We will now sketch some ideas regarding features to extract and how to perform object based classification in order to rule out marked objects with low confidence. The features and methods we present are preliminary, as we have just started with this activity. However, some test results are very promising.

5.1   Feature extraction

For each potential avalanche region from the segmentation module, several shape and context based features may be extracted. We propose to investigate:

- Maximum object length in averaged aspect direction. We expect that an avalanche has some extent in the aspect direction of the hill (Figure 5-1).
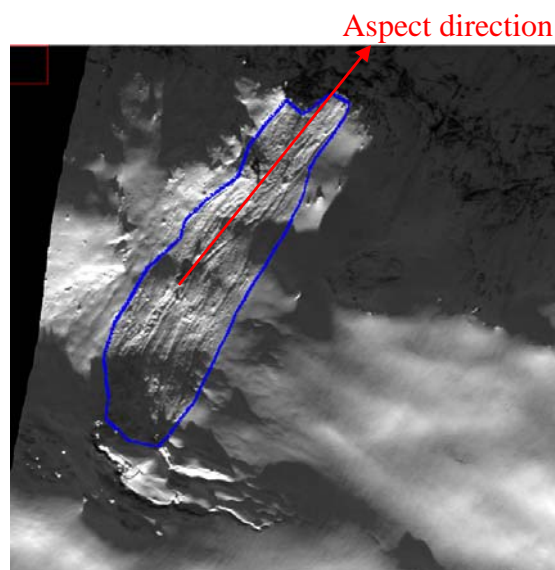
Figure 5-1: A typical avalanche stretched along the aspect direction of the hill.

- Complexity of shape (area/squared perimeter) is a descriptor of the avalanche shape, and we do not expect that this feature is very low.

- Number of nearby regions in the aspect direction.

- Distance to nearest avalanche in aspect direction. For each potential region, the distance and direction to all other segmented regions in the scene are calculated, and the distance to each region is calculated as (Solberg and Trier, 2009)

$$s = |\partial\theta| + a \cdot r,$$

where $\partial\theta$ is the direction differences, in radians, of the aspect direction and the direction to the neighbouring avalanche, *r* is the distance, in pixels, to the neighbouring avalanche region, and *a* is a constant to be determined.

- Area of avalanche region. Small regions are more likely to be noise; however, it might be part of an avalanche.

- GLCM features. As shown in Sec. 4.1, GLCM indeed provides some information about avalanche textures.

- Intensity. Avalanches occur in snow areas, and we expect that the intensity is large. However, some local adjustment may be necessary to suppress the effect of shadows.

- Orientation of avalanche region with respect to aspect. The avalanche in Figure 5-1 has an elliptical form with the major axis oriented along the aspect direction.

The proposed features are some suggestions, and it might be that other features are more efficient.

The calculated features are then stacked into a feature vector, which is the input to the classifier.

5.2   Classification

Using the proposed features in Sec. 5.1, the potential avalanche regions may be classified using a suitable classifier. Many methods may be used to construct the classifier, however, common for most classifiers are that they require some amount of feature vectors in the learning phase.

For only a few avalanches available, knowledge-based rules is recommended. Such rules are typically

       IF *region length in aspect dirction < threshold* **THEN** *remove region*

Many such rules may be constructed, resulting in a decision-tree, in which the output is detected avalanche regions. The design of a rule-based classifier is challenging, and care must be taken in order to construct a classifier that generalizes the classification problem sufficiently.

Alternatively, we may compute a *confidence score* for each region (Solberg and Trier, 2009). Hence, based on a multiple of the extracted features we estimate a score which expresses the strength of our belief that the region is an avalanche. Potential avalanche regions may be extracted by assigning a threshold to the confidence score, or we may just rank the regions based on our score. The strategy to use depends on the user requirements.

5.3   Estimating avalanche boundaries, connection, and labeling

After the classification stage, connection of detected avalanche regions is necessary. Here typically context based rules are applied. For instance, regions in the same path and close in distance may be assigned to the same avalanche. Furthermore, a re-estimation of the avalanche boundaries may be performed by growing the detected regions, under some context dependent rules.

6 Experimental results

6.1 Segmentation based on texture

The result of thresholding the entropy for the entire Hellesylt image is shown in Figure 6-2. Some close-up images of avalanches and the corresponding entropy thresholding result are shown in Figure 6-1, Figure 6-3, and Figure 6-4. Note that parts of some avalanches are not segmented out since we apply the forest mask in order to reduce the number of false avalanche detections.
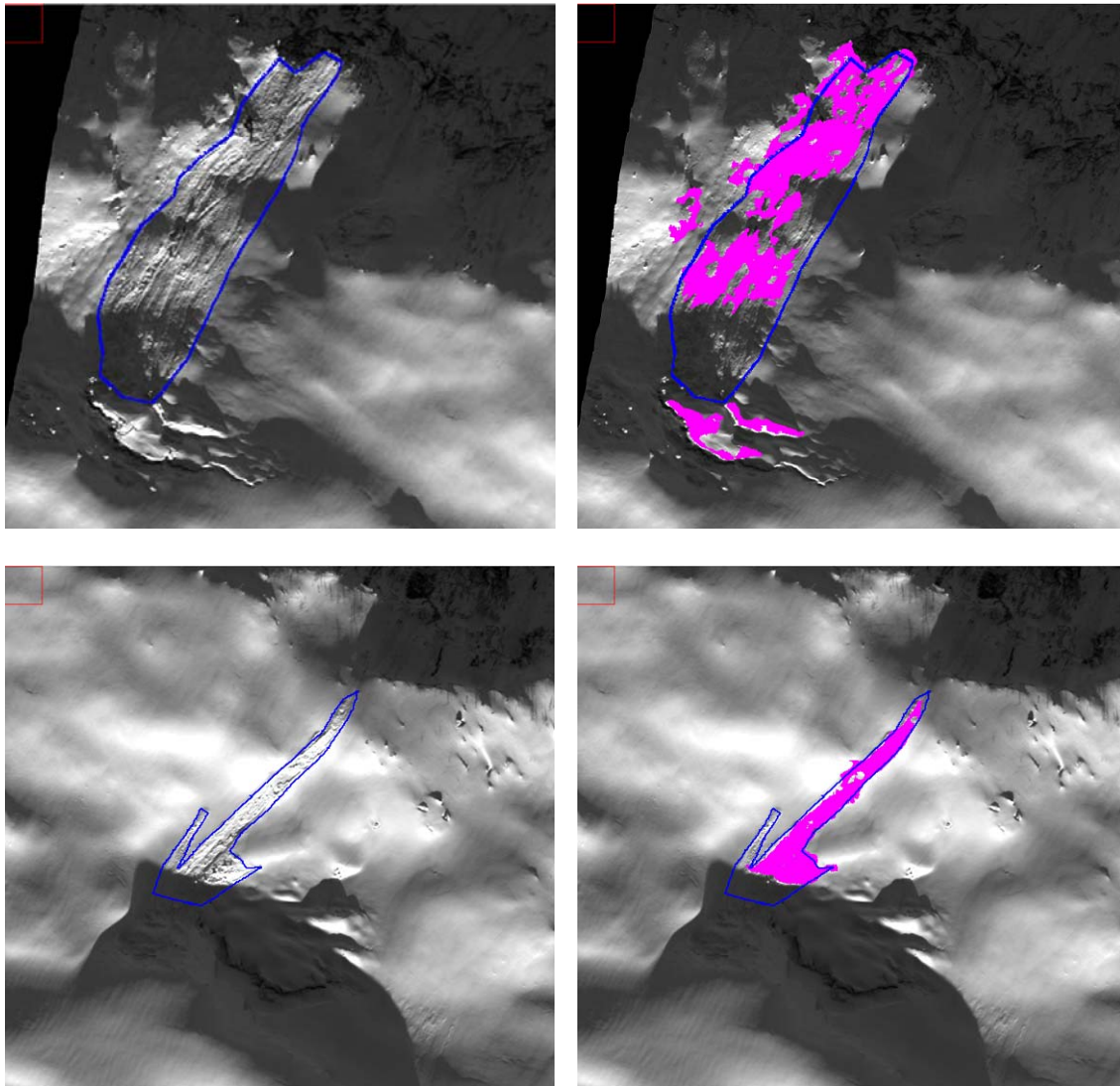
Figure 6-1. Two smaller avalanches (upper left corner of the Hellesylt image, see Figure 3-1). The avalanches are outlined in blue on the panchromatic image. On the right, high entropy segments overlay in pink.
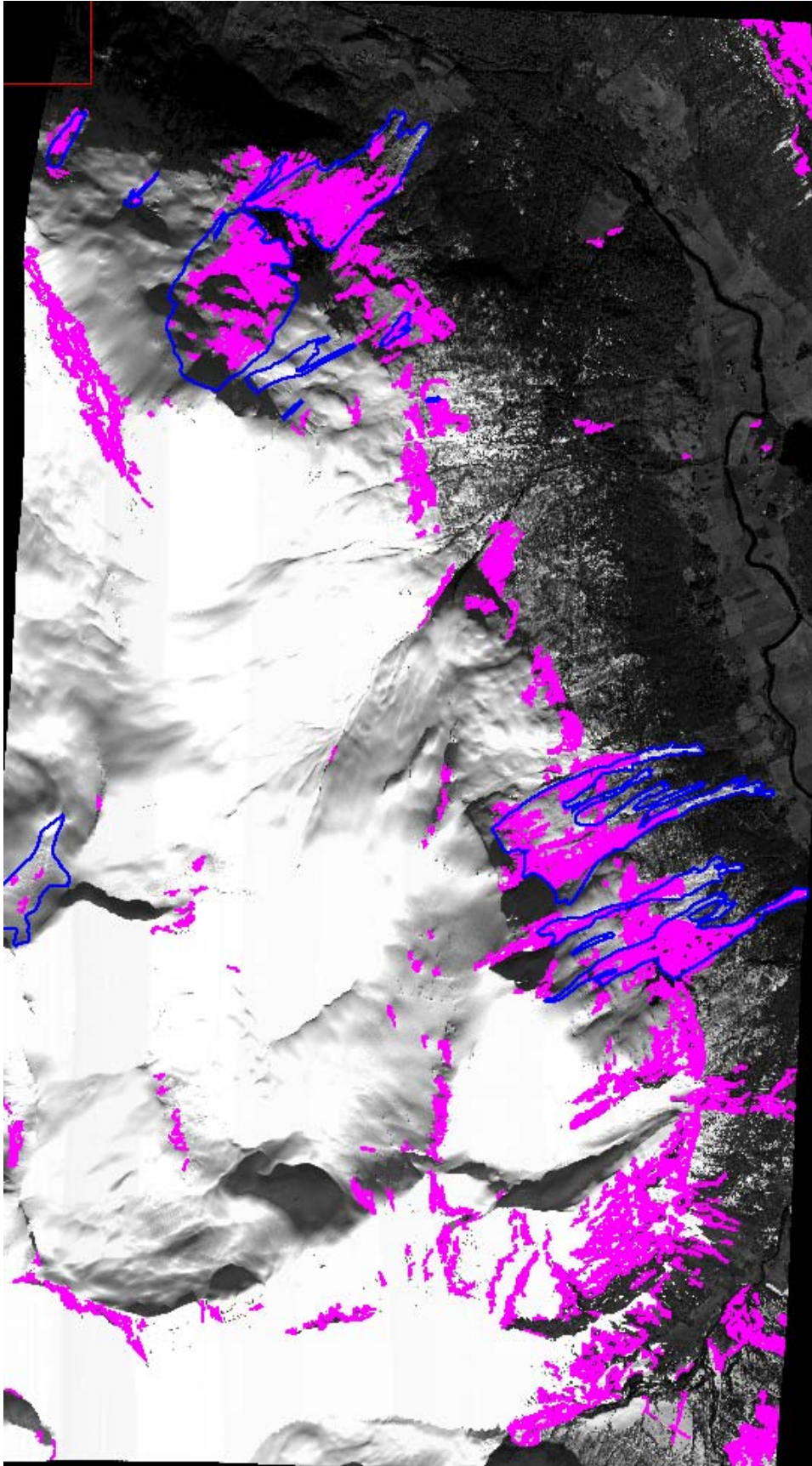
Figure 6-2. Result of thresholding the entropy image. Avalanches are outlined in blue. The pink segments are high entropy segments. Note that since we apply a forest mask in the detection algorithm, parts of some avalanches are masked out.

NR🌐   **Automatic detection of avalanches in high resolution satellite data**
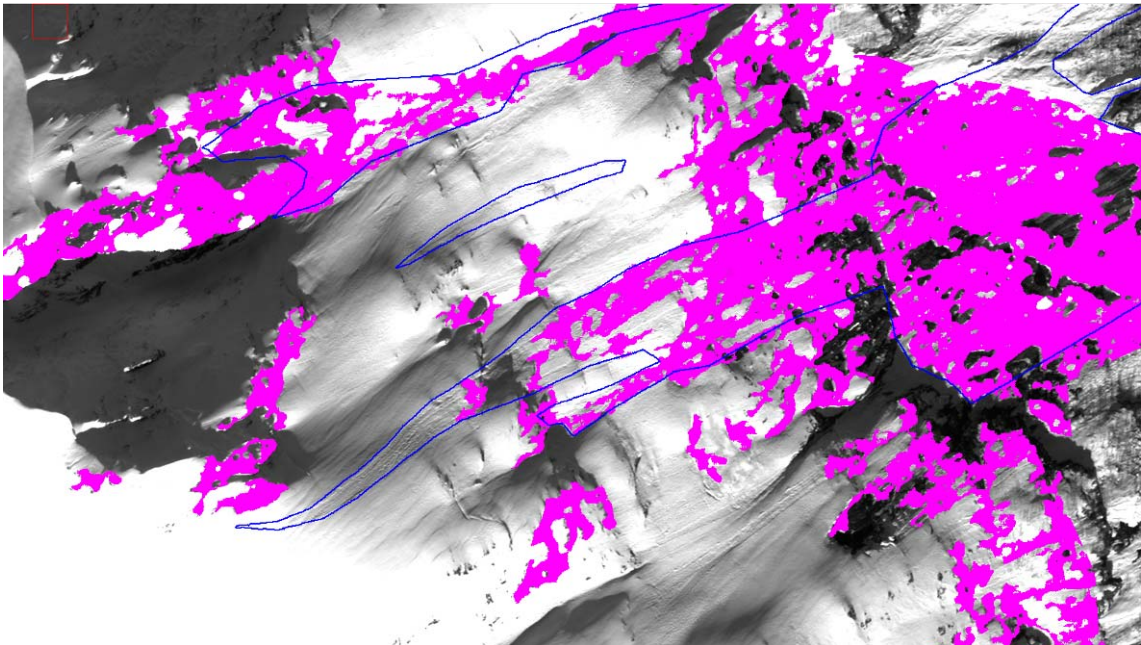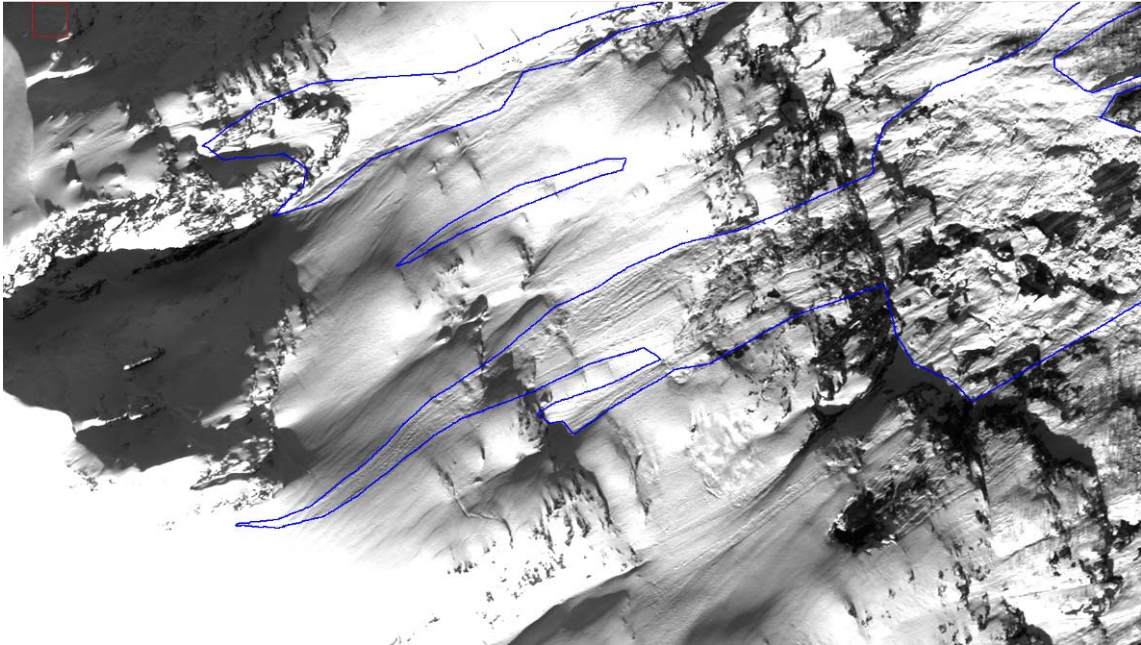
Figure 6-3. The starting zone area of two large avalanches in the lower right of the Hellesylt image (see Figure 3-1). The avalanches are outlined in blue, and the high entropy segments are shown in pink on the lower image.
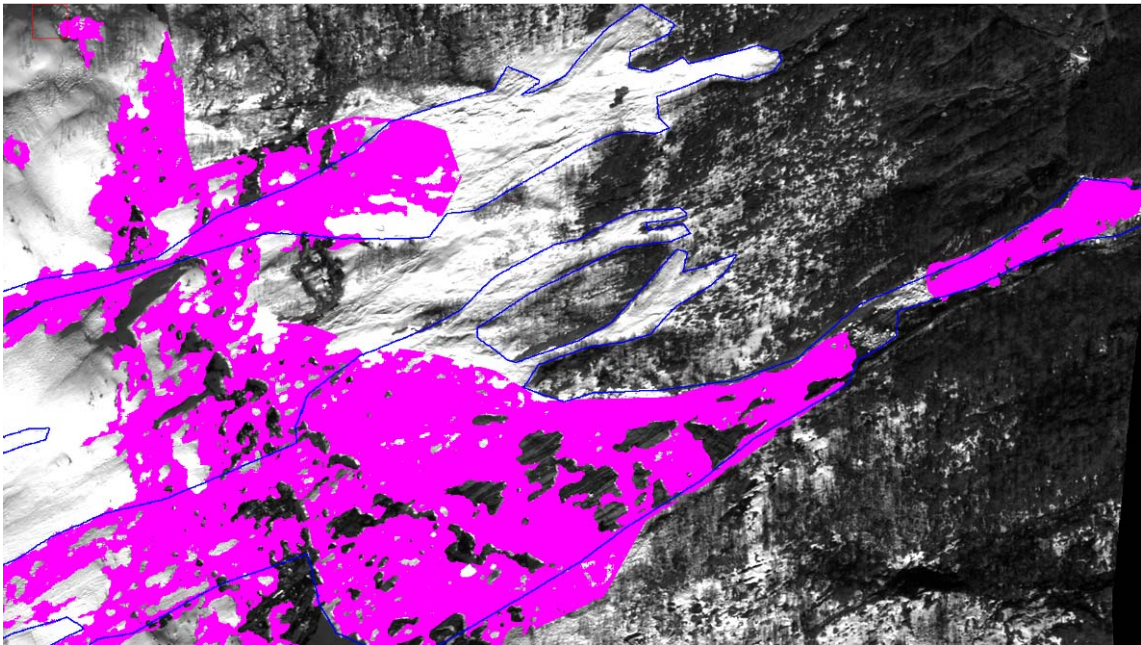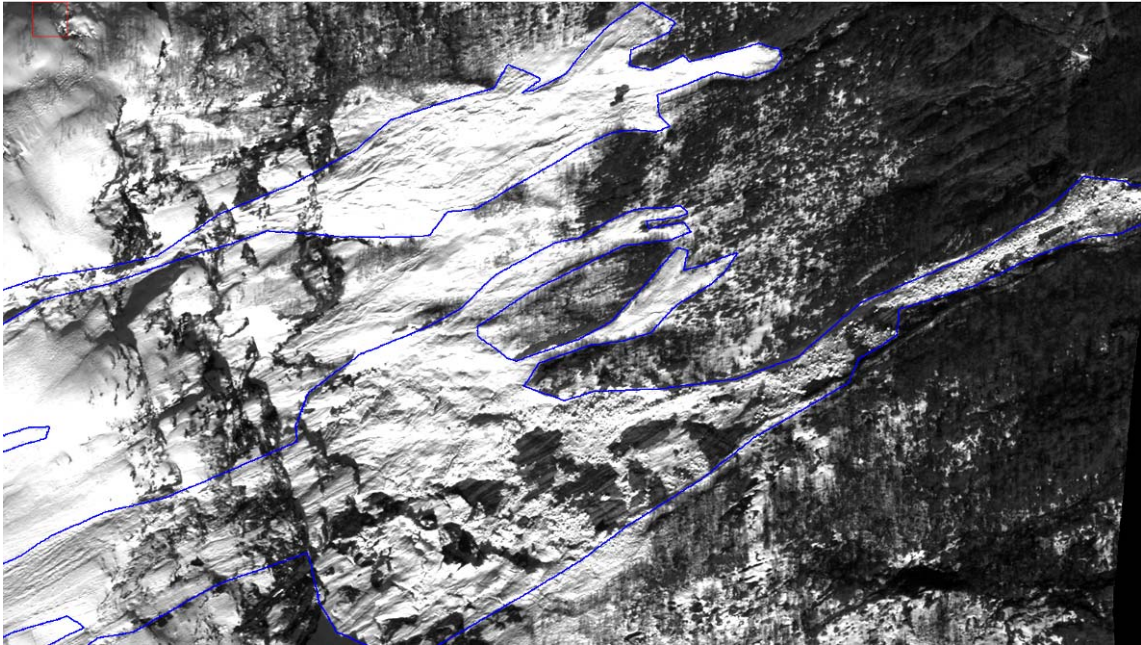
Figure 6-4. The run-out area of two large avalanches in the lower right of the Hellesylt image (see Figure 3-1). The avalanches are outlined in blue, and the high entropy segments are shown in pink on the lower image. Note that since we apply a forest mask in the detection algorithm, parts of the avalanche are masked out.

NR🌀 **Automatic detection of avalanches in high resolution satellite data**

6.2 Segmentation based on directional filters

The results of applying a filter bank on various regions are that various image features are enhanced depending on the type of filter applied (Figure 6-5). Typically, the avalanche is enhanced by applying the aspect directional filters whereas sparse trees are suppressed (Figure 6-5, mid figures). By applying the vertical directional filters, we obtain the opposite response (Figure 6-5, lower figures).

An overview of the segmented area of the Hellesylt image is shown in Figure 6-6, where red areas correspond to avalanche, green areas to smooth snow, blue areas to rugged snow, yellow areas to spares forest, and cyan areas corresponds to rock. Black areas are areas removed by the tree mask. The white lines are an outline of the avalanches. As in Figure 6-2 parts of the avalanches have not been segmented out since areas indicated by the tree mask are not considered. Some close-up images of avalanches and corresponding segmented areas are shown in Figure 6-7, Figure 6-8 and Figure 6-9.

Clearly the segmentation algorithm manages to extract areas corresponding to avalanches, and also manages to correctly segment areas corresponding to sparse trees. Some erroneous areas occur, but it is expected that they can be removed in the classification stage. Note also that the "fingers" in the large avalanches in the lower left of the Hellesylt image (Figure 6-6 and Figure 6-9) are not segmented since they are removed by the forest mask. The segmentation algorithm is not able to fully capture the shape of the avalanches, and some further improvements are necessary in order to fulfil that. Furthermore, the algorithm tends to mix shadowed areas with rock since both classes appear with low intensity values.

To visualize the power of one of the features, *length along aspect direction,* we have illustrated the segmented areas by assigning a gray level value corresponding to the feature value (Figure 6-10). However, from the image we also note that this feature is not sufficient in order to classify the segmented avalanche regions and multi-dimensional processing of the feature vectors are necessary.

6.2.1 Analysis of the validation image

The results of applying the directional filter method on the Dalsfjorden image, where the texton dictionary was learned from Hellesylt image worked very well (Figure 6-11 - Figure 6-14). As for the Hellesylt image, the algorithm extracted areas corresponding to avalanches and managed to separate spares forest and rugged snow from avalanches. Also for the Dalsfjorden image, the algorithm was not able to fully capture the shape of the avalanches.

The validation image contained many shadow areas that introduced erroneous classifications. Since the "rake" pattern was not present for some deposits; some avalanche deposits areas were not detected by the algorithm (Figure 6-13 and Figure 6-14).
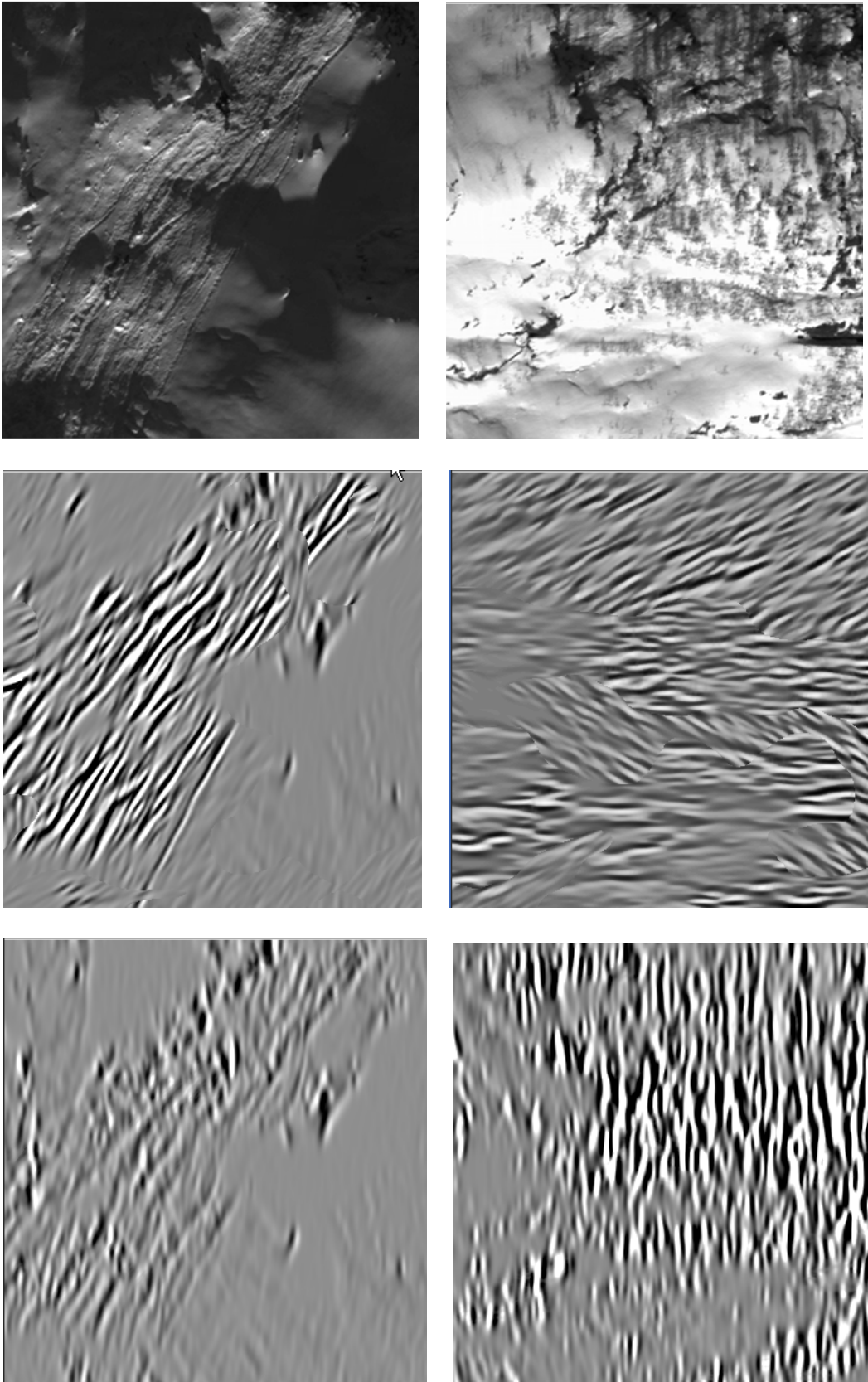
Figure 6-5: Left figures: Filter responses of a typical avalanche (upper left) filtered with a directional filter along aspect direction (mid figure left) and vertical direction (lower left). Right figures: Typical spares trees (upper right) filtered with direction filter along aspect direction (mid figure right) and vertical direction (lower right).

NR **Automatic detection of avalanches in high resolution satellite data**
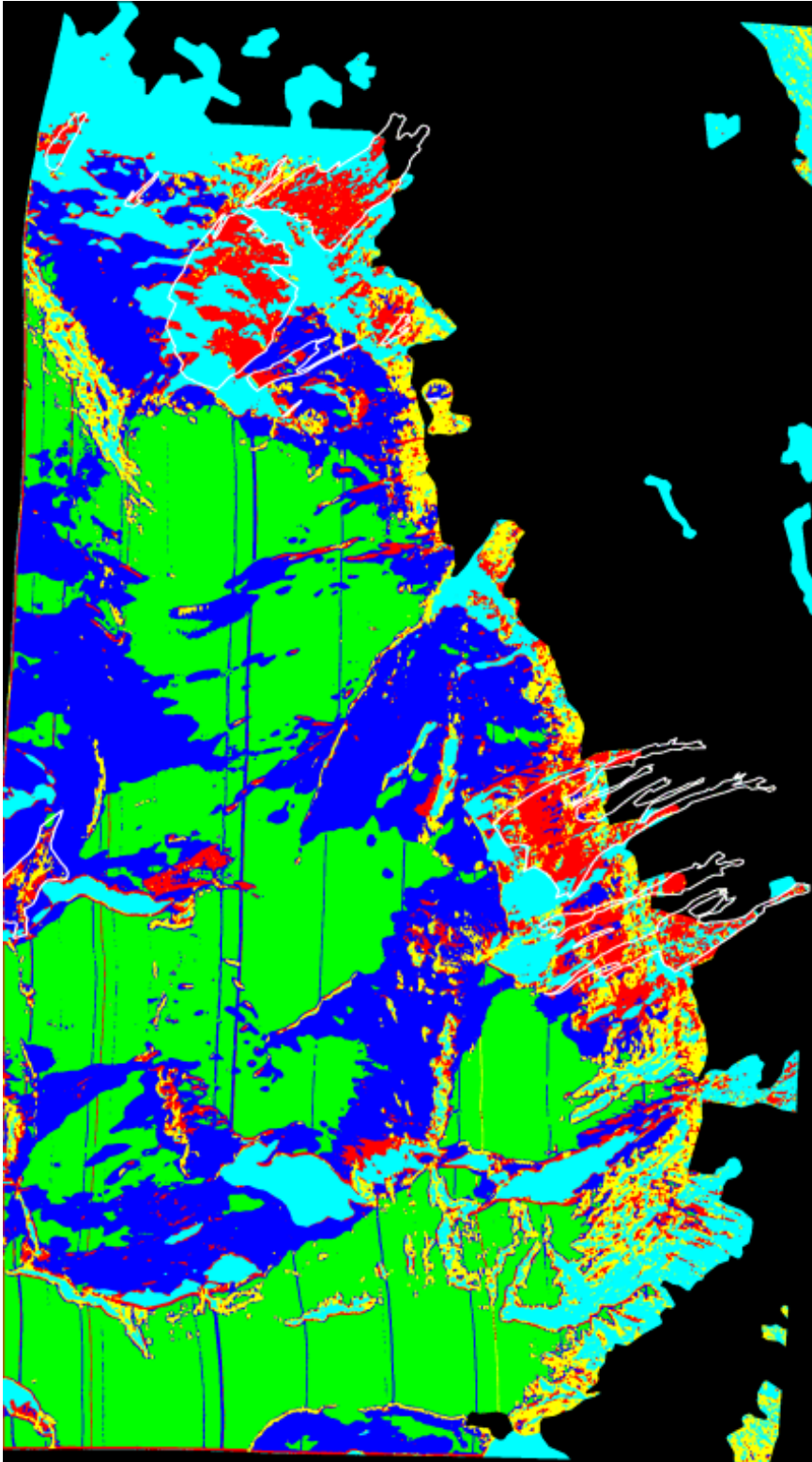
Figure 6-6. Segmented image Hellesylt. Red areas correspond to avalanches, green to smooth snow, blue to rugged snow, yellow to sparse trees, and cyan to rock. Black areas are areas removed by the forest and agriculture mask, and the white outlines are the avalanches.
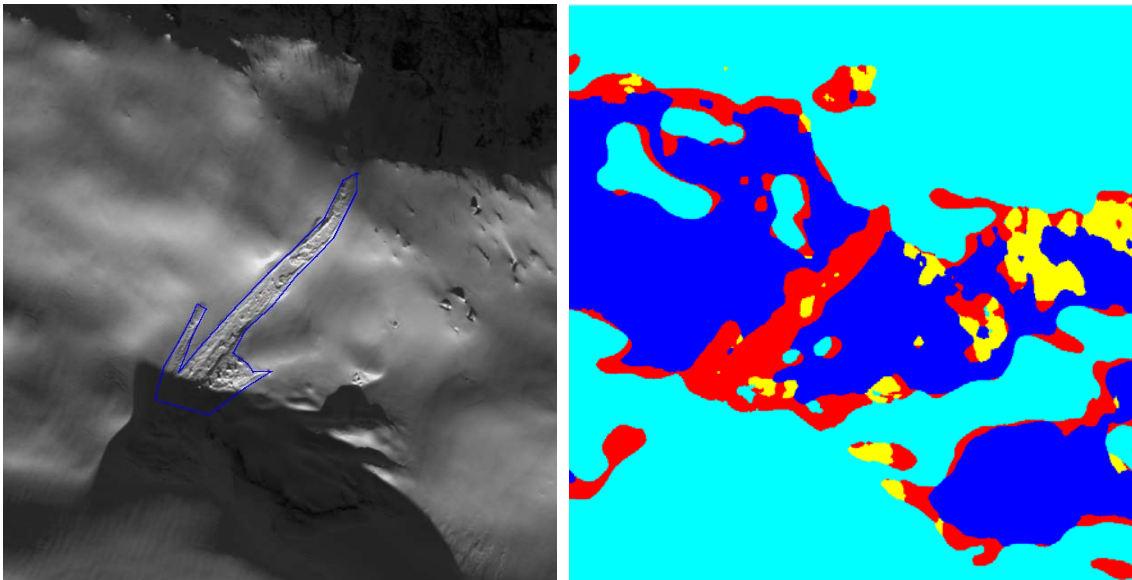
Figure 6-7: Example of detected avalanche in the Hellesylt image.
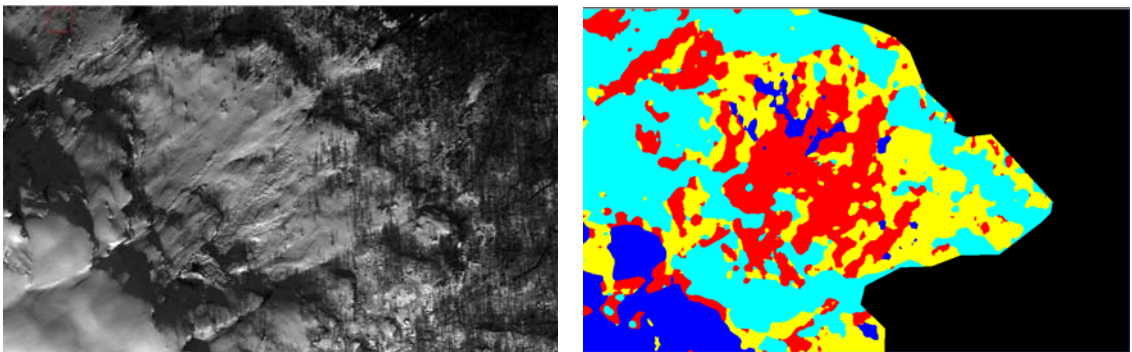
Figure 6-8: Example of detected avalanche near sparse forest in the Hellesylt image.
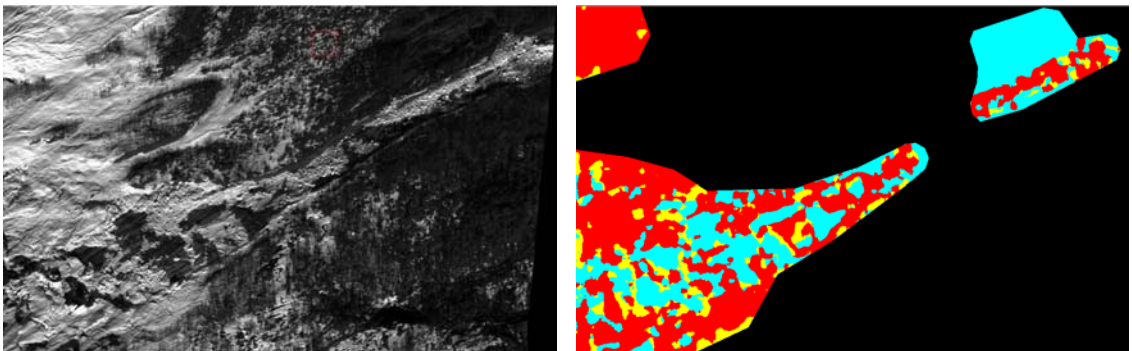
Figure 6-9: Example of detected avalanche close to forest area in the Hellesylt image. Note that the whole path of the avalanche is not segmented due to the forest mask.

NR   **Automatic detection of avalanches in high resolution satellite data**

Figure 6-10: Length along aspect image. Intensity corresponds to feature value.
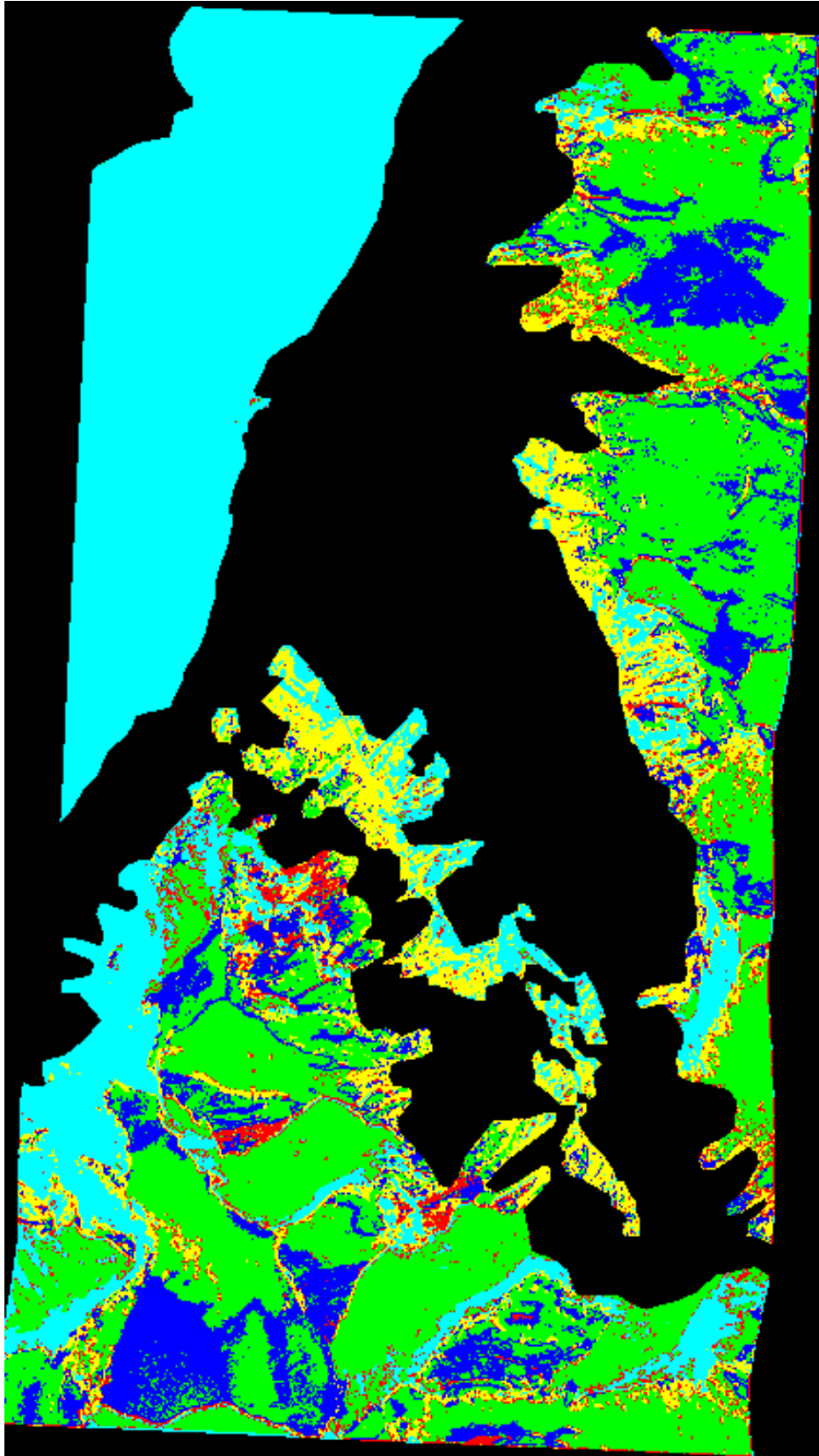
Figure 6-11: Segmented image Dalsfjorden. Red areas correspond to avalanches, green to smooth snow, blue to rugged snow, yellow to sparse forest, and cyan to rock. Black areas are areas removed by the forest and agriculture masks.

NR **Automatic detection of avalanches in high resolution satellite data**
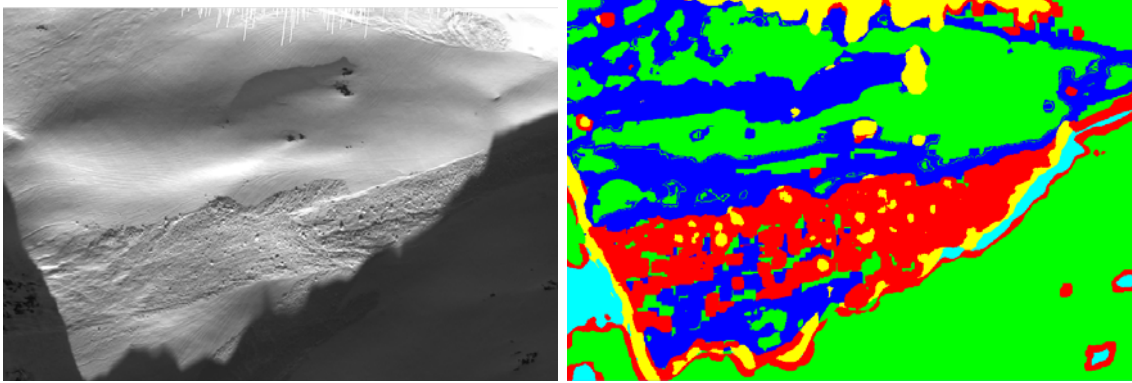
Figure 6-12: Example of detected avalanche in the Dalsfjorden image.
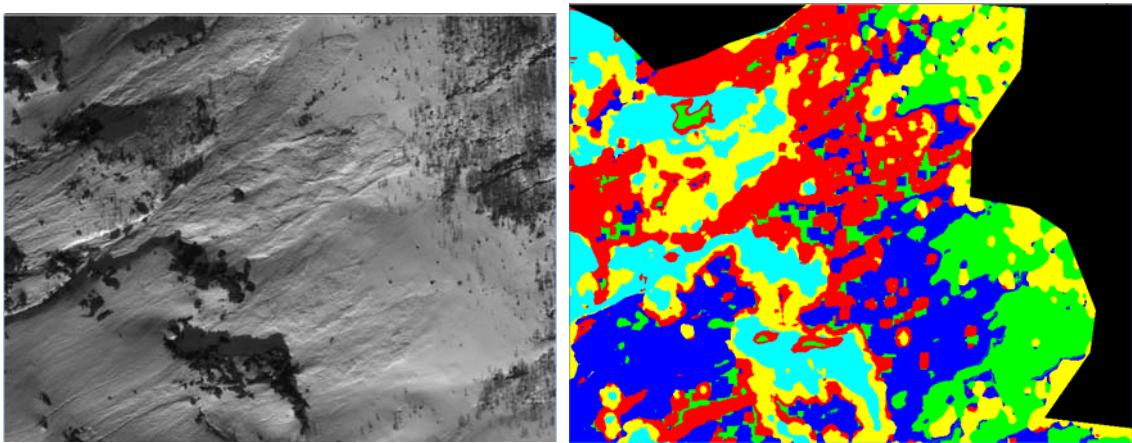
Figure 6-13: Example of detected avalanche in the Dalsfjorden image. Note that part of the avalanche deposit area has been classified to rugged snow.
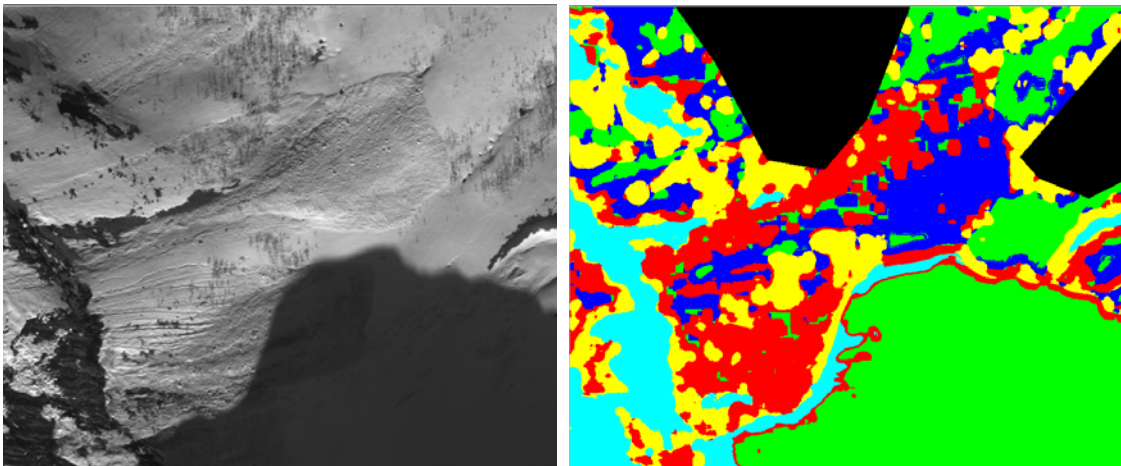
Figure 6-14: Example of detected avalanche in the Dalsfjorden image. Note that part of the avalanche deposit area has been classified to rugged snow.

7 Discussion and conclusions

The perhaps greatest challenge is to perform successful segmentation, i.e., to locate the image regions that correspond to potential avalanche sites. However, both GLCM and directional filter approaches were able to extract potential avalanche areas. The segmentation results indicate that the GLCM approach extracts the boundaries better than the directional filter approach, but struggles to separate sparse trees from avalanches. The strength of the directional filter approach is that it is able to separate sparse trees from avalanches well. The major drawback is that it often confuses shadowed areas with rock. Some further investigation is needed in order to process shadowed areas successfully.

The analysis of the validation image (Dalsfjorden) using the directional filter approach, where the texton dictionary was created from the Hellesylt image, performed in general very well. The algorithm was still able to detected avalanche areas in the image. Some challenges occurred due to many shadow areas in the validation images, and avalanche deposits without the characteristic "rake" pattern. These characteristics introduced some false alarms and non-detected avalanches. However, it is expected that a dictionary trained from several images would result correct classifications for such areas as well. It is not expected that the directional filter approach would work satisfactory if the validation image is covering a scene at another geographical location than the training image, since the vegetation and terrain may be completely different. However, this has not been explored yet.

It should also be considered to combine the two approaches, e.g., to include one or several GLCM features as input to the texton dictionary, and model the data base generation steps of the directional filtering approach. Actually, the directional filter segmentation approach described in Section 4.2 consists of two main steps: 1) construct bands that enhance the texture information content in the image by applying directional filters, and 2) use these bands as input to an algorithm that classifies each pixel, based on its image neighbourhood, to a texture class. The segments are then defined by grouping neighbouring pixels in the same texture class. By combining the two segmentation approaches we believe that some of the texture features produced from the GLCM matrices (Section 4.1) can be used as input to step 2) of the directional filter approach.

To extract the shape of the avalanche is a challenging task. A region growing method was suggested, but research needs to be conducted in order to find suitable criterions on how to grow the avalanche region. The directional filter bank approach applied a model based classification in order to classify a given pixel to one of the texture types. Other approaches may be better in order to define the regions, for instance by weighting the pixels in the neighbourhood of the pixel under investigation, or by applying a Markov random field as a means for introducing contextual information.

The resolution of the images has an impact of the quality of segmentation results. Some brief experiments indicated that for 2.4m resolution, the algorithms were more or less scalable, but for resolutions lower than that new methods or large adjustments of the methods were necessary.

In this work we have briefly demonstrated feature extraction of the mapped avalanche segments. By combining shape related features with context related features, such as number of

neighbouring objects, terrain aspect, etc., we believe that detection and mapping of avalanches could be successfully performed.

8 References

A. C. Bovik, M. Clark, and W. S. Geisler, 1990. Multichannel texture analysis using localized spatial filters. *IEEE Trans. Pattern Anal. Machin. Intell.,*vol. 12, no. 1, 55—72.

Y. Bühler, A. Hüni, M. Christen, R. Meister, and T. Kellenberger, 2009. Automated detection and mapping of avalanche deposits using airborne optical remote sensing data. *Cold Regions Science and Technology*, vol. 57, pp. 99-106.

I. Fogel and D. Sagi, 1989. Gabor filters as texture discriminators. *Biol. Cybern.,* vol. 61, 103—113.

A. K. Jain, N. K. Ratha and S. Lakshmanan, 1997. Object detection using Gabor filters, *Pattern Recogn.*, vol. 30(2), 293—309.

R. M. Haralick, K. Shanmugam, and I. Dinstein, 1973. Textural Features for Image Classification. *IEEE Trans. Systems, Man, Cybern.*, vol. 3, no. 6, pp. 610-621.

S.Ø. Larsen, H. Koren and R. Solberg, 2009. Traffic Monitoring Using Very-High-Resolution Satellite Imagery. *Photogrammetric Engineering and Remote Sensing*, vol. 75, 859-869.

R. Frauenfelder, K. Kronholm, 2010. avalRS - Remote sensing derived avalanche inventory data for decision support and hindcast after avalanche events. Deliverable 2: Service Demonstration Document. NGI Technical note TN 20081917-1: 20 pp.

A. Solberg, C. Brekke and P. Husøy, 2007. Oil spill detection in Radarsat and Envisat SAR images, *IEEE Trans. Geosci. Remote Sens.*, vol. 45, 746-755.

A. Solberg and Ø. D. Trier, 2009. SatHavOlje: Improvements during the 2008 project. *NR Note*, Norwegian Computing Center, SAMBA/01/09.

Ø.D. Trier, S.Ø. Larsen and R. Solberg, 2009. Automatic detection of circular structures in high-resolution satellite images of agricultural land. *Archaeological Prospection*, vol. 16, 1-15.

M. Varma and A. Zisserman, 2004. A statistical approach to texture classification from single images. *Int. J. Computer Vision: Special Issue on Texture Analysis and Synthesis*, vol. 62(1-2), 61—81.